

# Model-updated Image-guided Liver Surgery: Preliminary results using Intra-operative surface characterization

Prashanth Dumpuri<sup>1</sup>, Logan W. Clements<sup>2</sup>, Benoit M. Dawant<sup>3,1a</sup>, Michael I. Miga<sup>1a</sup>

<sup>1</sup>Vanderbilt University, Department of Biomedical Engineering, Nashville, TN 37235

<sup>2</sup>Pathfinder Therapeutics, Inc., Nashville, TN 37204

<sup>3</sup>Vanderbilt University, Department of Electrical Engineering and Computer Science, Nashville, TN 37235

{prashanth.dumpuri, michael.i.miga, benoit.dawant}@vanderbilt.edu  
lwc@2pti.com

## ABSTRACT

The current protocol for image-guidance in liver surgeries involves rigid registration algorithm. Systematic studies have shown that the liver can deform up to 2cms during surgeries thereby compromising the accuracy of the surgical navigation systems. Compensating for intraoperative deformations using computational models has shown promising results. In this work, we follow up the initial rigid registration with a computational approach. The proposed computational approach relies on the closest point distances between the undeformed pre-operative surface and the rigidly registered deformed intra-operative surface. We also introduce a spatial smoothing filter to generate a realistic deformation field using the closest point distances. The proposed approach was validated in both phantom experiments and clinical cases. Preliminary results are encouraging and suggest that computational models can be used to improve the accuracy of image-guided liver surgeries.

**Keywords:** Image-guided liver surgery, Finite element analysis, linear elastic model, Liver deformation, Image registration

## 1. INTRODUCTION

Image-guided surgery has been used with success in the treatment of brain tumors, breast cancer and more recently in deep brain stimulations. These advancements in medical imaging have only been recently translated to open abdominal surgeries and partial hepatectomies. As in other image-guided surgical applications, image-guidance in open abdominal surgeries relies on the establishment of an accurate relationship between the patient's pre-operative image space and the intra-operative organ space/physical space. This process of establishing a relationship between the image-space and the physical-space is known as registration. The current protocol for registration in partial hepatectomies involves an initial pose estimation provided by a point based registration of anatomical landmarks which is then improved by using rigid surface registration techniques which use the pre-operative surface segmented from the diagnostic images and the exposed intra-operative surface [9, 6]. While these image-to-physical space alignments are relatively straightforward, non-rigid tissue deformation (also known as intra-operative shift) during hepatectomies compounds the procedure and compromises the accuracy of guidance systems that rely on the aforementioned rigid registration techniques. The existing methods for intra-operative shift compensation can be classified into two main categories: (i) Intra-operative imaging techniques such as intra-operative magnetic resonance (iMR) and intra-operative computed tomography (iCT) imaging, intra-operative ultra-sound (iUS) and (ii) computational modeling. While iMR techniques have shown promise for complex hepatic surgeries [1] so far it has been limited to research institutions. Though iUS is used during hepatic surgeries more often than not iUS provides poor resolution images.

Computational models have been used to compensate for shift in neurosurgeries [11, 8, 7] and are relatively new to the field of hepatectomies and liver surgeries. Recently, we proposed an approach [5] utilizing a template of pre-operatively computed model solutions in the context of partial hepatectomies. The success of the algorithm proposed by us in [5] relies on the assumption that it is possible to account for all possible forces that cause the liver to shift/deform during hepatectomies. However our anecdotal observations in the operating room have shown that the

---

<sup>a</sup> Michael I. Miga and Benoit M. Dawant are co-founders of Pathfinder Therapeutics Inc.

surgeon manipulates and mobilizes the liver in a manner he/she chooses fit to get better access to the tumor causing random deformations to the liver. These observations point out that it is highly improbable to account for all possible forces that cause the liver to deform during surgery. Therefore, in this work we propose a “direct” approach to account for the intra-operative shift by combining a cheap and efficient intra-operative imaging method with a computational model. The proposed algorithm relies on the acquisition of a three-dimensional representation of the exposed intra-operative surface. In that context, we use a commercially available laser range scanner and we have demonstrated in the past that this scanner can be used to acquire intra-operative surfaces during brain tumor resection therapies [10] and liver surgeries [4]. The proposed algorithm has been evaluated in a series of phantom experiments and two patients undergoing partial hepatectomies at two different clinical sites. Quantitative and qualitative results have been presented in the Section 4.

## 2. METHODS

### 2.1 Computational Model

In this work, we assume the liver to be an isotropic solid with a linear stress-strain relationship, governed by the following equation:

$$\nabla \circ \sigma = B \quad (1)$$

where  $\sigma$  represents the stress tensor and  $B$  the external forces acting on the object. Since we assume the liver to have a linear relationship between stress and strain,  $\sigma = C\epsilon$  where  $C$  represents the material stiffness matrix and is dependent on Young’s modulus ( $E$ ) and Poissons ratio ( $\nu$ ). Using Galerkin weighted residuals and linear basis functions to solve the above equation, the system of equations to solve displacements  $\{u\}$  at every node in the tetrahedral mesh can be represented as

$$[K] \{u\} = \{B\} \quad (2)$$

The first step in using the computational model is to segment the liver from the patient’s abdominal scan and create a marching cubes description of the surface. This surface is then fed to a tetrahedral mesh generator which creates a three-dimensional volumetric mesh of the patient’s liver. A key component to any computational model/finite element model is the application of forces (also known as boundary conditions) that are used to drive the model and predict intra-operative shift. This part of our algorithm has been discussed in detail in Section 2.3.

### 2.2 Initial Rigid Alignment of the intra-operative liver surface to the pre-operative images

A successful image-space to physical-space alignment is critical for this work and this section describes in brief the rigid surface registration technique used to align the exposed intra-operative surface to the pre-operative image sets. Our group has been researching the incorporation of a commercially available laser range scanner to acquire three-dimensional surfaces of the exposed liver during surgery [4]. Initial attempts at establishing image-space to physical-space relationships in our group focused on using the standard iterative closest point algorithm (ICP) [2] to rigidly register the surface acquired using laser range scanner to the pre-operative liver surface (obtained via segmentation from the patient’s diagnostic images). Clements et al. [6] reported an approach using weighted salient anatomical features to increase robustness of the rigid surface registrations. These salient anatomical features are identifiable in both the pre-operative image set and the intra-operative surface acquired using the laser range scanner. Falciform ligament (which divides the left and right lobes of the liver) and the inferior ridges are good examples of such anatomical features. These features are used to bias the point correspondence estimation in the traditional ICP algorithm. Clements et al. [6] demonstrated the robustness of this weighted feature ICP algorithm in a series of phantom experiments and also demonstrated that this algorithm performed better than the point-based registration algorithms and the traditional ICP algorithm in a series of clinical cases. Figure 1 shows an example registration obtained using the weighted patch ICP algorithm. Figure 1a shows the pre-operative surface segmented from the diagnostic images and the salient features identified on the segmented surface. Figure 1b shows the intra-operative surface obtained using the laser range scanner and the salient anatomical features identified on that surface. Figure 1c shows the registered intra-operative surface overlaid on the pre-operative liver surface.

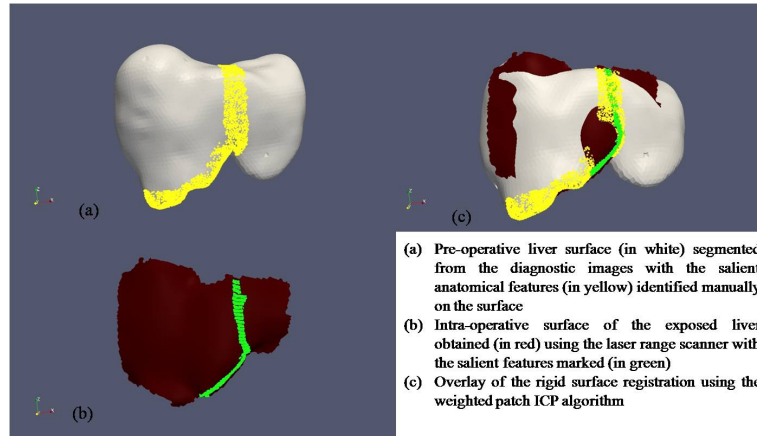


**Figure 1.** Example result of the rigid registration reported in [6]. Note how the salient anatomical features align after registration (in Figure 1c).

### 2.3 Improve the rigid alignment using a computational model

Once the rigid alignment has been established we use the closest point distances between the registered intra-operative surface and the pre-operative liver surface to guide the application of boundary conditions necessary to drive the computational model described in Section 2.1. Figure 2 shows an example of the closest point distances between the registered intra-operative surface and the patient's pre-operative surface. It should be noted that the two surfaces were aligned using the weighted patch ICP algorithm. Positive values in the figure indicate the weighted patch ICP algorithm places the intra-operative surface to be on top of the pre-operative surface and negative values indicate that the algorithm positions the intra-operative surface underneath the pre-operative surface.

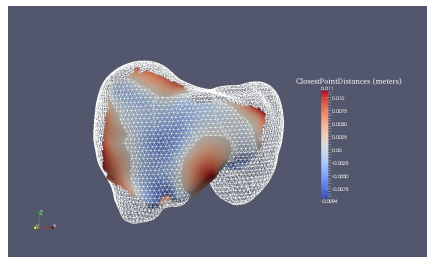


**Figure 2.** Example result of closest point distances (in meters) between the registered intra-operative surface and the pre-operative surface. Registration was performed using the rigid registration algorithm reported in [6]. Positive values mean that the intra-operative surface is on top of the pre-operative surface and negative values indicate that the intra-operative surface is underneath the pre-operative surface.

It can also be seen from the figure that these closest point distances are sparse in nature. In other words these distances are available just for a few nodes on the finite element mesh. The proposed algorithm uses a smoothing filter based on spatial connectivity between the nodes to smooth the closest point distances to flanking nodes/nodes outside the extent covered by the intra-operative surface. Given a rigid alignment between the pre-operative surface and the intra-operative liver surface and a three dimensional tetrahedral volumetric mesh, the algorithm proceeds as follows:

**Step 1.** Obtain signed closest point distances between the nodes in the three-dimensional finite element and the rigidly registered intra-operative surface. It should be noted that these distances exist only for nodes that are covered by the spatial extents of the registered intra-operative surface. Nodes that lie outside are assigned a zero value for the closest point distances.

**Step 2.** Establish a radius of connectivity for every node on the finite element mesh and use that connectivity to generate an average distance by summing all the closest point distances from the previous step. Therefore in flanking regions (regions outside the spatial extents of the registered intra-operative surface) zero's are part of

that average and therefore the distances computed in this step are lesser than the ones computed in the previous step. A signed distance value is thus computed for every surface node in the finite element mesh.

**Step 3.** The distance that is calculated in step 2 for each node is thought of as a displacement boundary condition occurring normal (i.e. perpendicular) to the organ surface.

**Step 4.** These displacement boundary conditions are applied to the computational model described in Section 2.1 and a volumetric deformation field is computed using Equation 2.

**Step 5.** The volumetric deformation field is used to deform the finite element mesh and steps 1 through 4 are repeated till the average closest point distances between the registered intra-operative surface and the pre-operative surface lies below a threshold value.

The algorithm was tested in a series of phantom experiments and four patients undergoing partial hepatectomies at four different clinical sites and results have been presented in Section 4.

### 3. DATASETS USED FOR VALIDATION

#### 3.1 Phantom Validation

A series of phantom experiments were performed using a liver phantom created using Smooth-On Ecoex 00-10 (Smooth-On, Easton, PA). The phantom was rigidly attached to a plexiglass base using a Teflon screw. Seven Teflon spheres surrounding the phantom were affixed at varying heights to the plexiglass base. Forty-three stainless steel beads were distributed randomly in the phantom to serve as sub-surface targets for error computation. A stripe of white paint was placed on the phantom in the falciform ligament region to facilitate the delineation of this salient anatomical feature. Computed tomography (CT) scans of the phantom were obtained in the undeformed state. These scans were used to generate (a) the pre-operative surface for rigid alignment and (b) the volumetric tetrahedral mesh used for the computational model. Deformation then imposed on the phantom using a surgical towel underneath the inferior ridge of right lobe. Surface of the deformed state were acquired using a CT scan and a laser range scanner (LRS) from RealScan 200C, 3-D Digital Corporation, Bethel, CT Surfaces. It should be noted that the surface acquired by the laser range scanner was a partial surface description of the anterior part of the phantom. Figure 3 shows the experimental set up. Figure 3a shows the deformation applied to the right lobe of the phantom and Figure 3b shows the distribution of 43 sub-surface stainless beads.

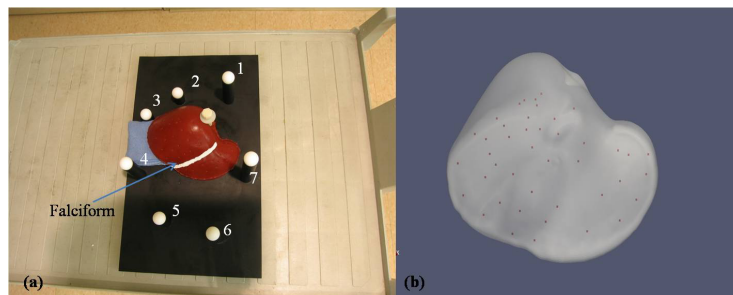


**Figure 3.** (a) Experimental set-up for the phantom datasets. Deformation was applied using a surgical towel placed underneath the right lobe. A white stripe was painted in the falciform region to facilitate the delineation of that salient anatomical feature. Seven Teflon spheres that surround the phantom were used as landmarks for point-based registration. (b) Distribution of the 43 stainless beads that serve as sub-surface targets for error computation.

Teflon spheres that surround the phantom were localized in the CT and LRS datasets served as landmarks for point-based registration. The deformed surfaces were initialized using this point-based registration and then aligned to their undeformed counterpart using the weighted patch algorithm described in [6]. The computational algorithm described in Section 2.3 was then used to improve this rigid surface alignment. Sub-surface target errors were computed for the rigid point-based registration, weighted patch ICP registration and the computational model and results have been presented in the following section.

#### 3.2 Clinical Validation

Two patients undergoing partial hepatectomies were selected randomly from a 75 patient clinical conducted by Pathfinder Therapeutics Inc. Patient 1 underwent the hepatectomy at University of Pittsburgh Medical Center and Patient 2 at Memorial Sloan Kettering Cancer Center. Surface and volumetric tetrahedral mesh were generated from the undeformed pre-operative diagnostic images and intra-operative surfaces were acquired using the laser range scanner described above. Four anatomical landmarks were identified on the pre-operative CT images and on the intra-operative surface using a tracked pen probe. A point-based registration was performed using these four

landmarks to establish an initial alignment. The surfaces were then rigidly registered similar to the phantom experiments and the computational algorithm was used to improve the rigid alignment. Since sub-surface targets were not available for the clinical cases, closest point distances between the undeformed and rigidly registered surfaces were compared to the closest point distances between the undeformed surface and the model predictions and have been reported in the following section.

## 4. RESULTS

### 4.1 Results for Phantom experiments

Table 1 reports the errors at the forty-three sub-surface stainless beads that were used as targets. Column 2 in the table reports the target registration error (TRE) for the point-based registration using the Teflon spheres that surrounded the phantom. Column 3 reports the TRE using the weighted patch algorithm and Column 4 reports the error between the model predicted positions for the sub-surface targets and those that were predicted using the weighted patch ICP registration.

**Table 1.** Target registration errors for the rigid registration algorithm (Columns 2 and 3) and the proposed computational approach (Column 4)

Deformation	Post-PBReg	Post-wICP	Post-Model
	(mm)	(mm)	(mm)
<b>Right - Full Surface</b>	22.8±8.8(42.3)	2.7±1.6(6.7)	0.6±0.5(1.8)
<b>Right - Partial Surface</b>	22.8±8.8(42.3)	4.5±2.1(10.0)	3.0±2.1(8.1)

Table 1 shows that the model outperforms the rigid registration algorithm by 78% when the entire deformed surface is used to drive it and it outperforms the rigid registration algorithm by 33% when the partial surface description from the LRS is used.

### 4.2 Results for Clinical Cases

Table 2 reports closest point distances after rigid registration (row 1) and model prediction (row 2). Averaging over both patient cases, the model improves the closest point distances after rigid registration by 64%

**Table 2.** Closest point distances after rigid registration (Row 1) and the proposed computational approach (Row 2). Patient 1 underwent a partial hepatectomy at University of Pittsburgh Medical Center and Patient 2 underwent the surgery at Memorial Sloan Kettering Cancer Center

	Patient 1	Patient 2
	(mm)	(mm)
<b>wICP</b>	4.8±3.9 (24.3)	3.9±2.6 (11.3)
<b>Model</b>	1.9±3.0 (20.0)	1.3±0.9 (7.1)

## 5. DISCUSSION

Previous studies have demonstrated reasonable success in using closest point distances to predict intra-operative deformations during liver surgeries [3] and brain tumor resection therapies [8]. There are two important features that distinguish the proposed algorithm from the aforementioned studies: (i) we use sparse intra-operative data used to drive the computational model. In other words, the closest point distances between the registered intra-operative surface and the pre-operative liver surface are available just for a few nodes on the surface of the brain and, (ii) the spatial averaging filter allows us to approximate boundary conditions for regions where intra-operative data is not acquired. The spatial averaging filter also ensures that the closest point distances between the registered intra-operative surface and the pre-operative liver surface are applied in an incremental fashion, thereby preventing unrealistic deformations.

Sub-surface targets were not available for the clinical cases reported here and therefore closest point distances between the undeformed and deformed surfaces were used to measure accuracy of the proposed approach. Since surgeons are more concerned with the sub-surface vasculature it should be noted that the closest point distances between the surfaces is not a reliable metric. We have acquired post-operative scans and are currently investigating the appropriateness of using sub-surface vessels as targets for the proposed approach.

An interesting observation from the results reported for the phantom experiments is that the proposed computational approach performs significantly better when the entire deformed surface is available to drive the model. Given that we do not have access to iCT and iMR techniques, an entire surface description of the deformed intra-operative surface is not available to us. We are limited to partial surface descriptions acquired using a laser range scanner. The results presented for the phantom experiments in Table 2 suggest that there is a modest improvement (about 33%) when using partial surfaces with the computational approach. It should however be noted that the computational approach relies on the closest point distances between the undeformed and deformed surface after rigid alignment. Therefore, it is reasonable to assume that increasing the accuracy of the rigid registration algorithm will affect the outcome of the computational approach. We are currently investigating methods to improve the accuracy of the weighted patch algorithm. There is however no doubt that the model outperforms the rigid registrations and preliminary results not presented here show that the computational approach is compatible with the surgical time constraints. Given this, we are highly encouraged by the results presented here and are working on improving the accuracy of the proposed approach. Once we establish the fidelity of the proposed approach in more clinical cases, we also plan to update the pre-operative images using the deformation field predicted by the computational approach and compare these updated images to the post-operative scans.

## **6. CONCLUSIONS**

Preliminary results reported here indicate that a registration algorithm followed by the proposed computational approach improves the accuracy of guidance during liver surgeries. The proposed approach needs to be validated in more clinical cases before it can be used in the operating room.

## **ACKNOWLEDGEMENTS**

This work has been supported by National Institute of Health, Grant # R21 EB007694-01 and National Cancer Institute Grant # CA119502. The authors would like to thank Dr. Robert L. Galloway for his valuable inputs.

## REFERENCES

- [1] Oliver F Bathe, Houman Mahallati, Francis Sutherland, Elijah Dixon, Janice Pasieka, and Garnette Sutherland. Complex hepatic surgery aided by a 1.5-tesla moveable magnetic resonance imaging system. *Am J Surg*, 191(5):598–603, May 2006.
- [2] P. J. Besl and N. D. McKay. A method for registration of 3-D shapes. *IEEE Trans. Pattern Anal. Mach. Intell.*, 14(2):239–256, 1992.
- [3] D. M. Cash, M. I. Miga, T. K. Sinha, R. L. Galloway, and W. C. Chapman. Compensating for intraoperative soft-tissue deformations using incomplete surface data and finite elements. *IEEE Trans. Med. Imaging*, 24(11):1479–1491, Nov. 2005.
- [4] D. M. Cash, T. K. Sinha, W. C. Chapman, H. Terawaki, B. M. Dawant, R. L. Galloway, and M. I. Miga. Incorporation of a laser range scanner into image-guided liver surgery: Surface acquisition, registration, and tracking. *Med. Phys.*, 30(7):1671–1682, Jun 2003.
- [5] L. W. Clements, P. Dumpuri, W. C. Chapman, Jr. R. L. Galloway, and M. I. Miga. Atlas-based method for model updating in image-guided liver surgery. In *Medical Imaging 2007: Visualization and Image-Guided Procedures*, volume 6509, 2007.
- [6] Logan W Clements, William C Chapman, Benoit M Dawant, Robert L Galloway, and Michael I Miga. Robust surface registration using salient anatomical features for image-guided liver surgery: algorithm and validation. *Med Phys*, 35(6):2528–2540, Jun 2008.
- [7] P. Dumpuri, R. C. Thompson, B. M. Dawant, A. Cao, and M. I. Miga. An atlas-based method to compensate for brain shift: Preliminary results. *Medical Image Analysis*, Accepted, 2006.
- [8] M. Ferrant, A. Nabavi, B. Macq, F.A. Jolesz, R. Kikinis, and S.K. Warfield. Registration of 3-D intraoperative mr images of the brain using a finite-element biomechanical model. *IEEE Transactions on Medical Imaging*, 20(12):1384–1397, 2001.
- [9] A. J. Herline, J. L. Herring, J. D. Stefansic, W. C. Chapman, R. L. Galloway Jr., and B. M. Dawant. Surface registration for use in interactive, image-guided liver surgery. *Comput. Aided Surg.*, 5(1):11–17, 2000.
- [10] T. K. Sinha, B. M. Dawant, V. Duay, D. M. Cash, R. J. Weil, R. C. Thompson, K. D. Weaver, and M. I. Miga. A method to track cortical surface deformations using a laser range scanner. *IEEE Trans. Med. Imaging*, 24(6):767–781, June 2005.
- [11] O. Skrinjar, D. Spencer, and J. Duncan. Brain shift modeling for use in neurosurgery. In *LNCS: Medical Image Computing and Computer-assisted Intervention: MICCAI '98*, volume 1496, pages 641–649. Springer-Verlag, 1998.